Model for Corrosion of Carbon Steel in Lithium Bromide Absorption Refrigeration Systems

*A. Anderko and R.D. Young**

ABSTRACT

A comprehensive model has been developed for the computation of corrosion rates of carbon steels in the presence of lithium bromide (LiBr)-based brines that are used as working fluids for absorption refrigeration cycles. The model combines a thermophysical module that provides realistic speciation of aqueous systems with an electrochemical module for partial cathodic and anodic processes on the metal surface. The electrochemical module includes the adsorption of halides, which strongly influences the corrosion process. Also, the model takes into account the formation of passive films and their interactions with solution species. The model has been verified by comparing calculated corrosion rates with laboratory data for carbon steels in LiBr solutions. Good agreement between calculated and experimental corrosion rates has been obtained. In particular, the model is capable of reproducing effects of pH-adjusting components and selected inhibitors on the rates of general corrosion. The model has been incorporated into a program that makes it possible to analyze effects of various conditions such as temperature, pressure, solution composition, or flow velocity on corrosion rates.

KEY WORDS: electrochemical kinetics, inhibitors, lithium bromide, modeling, prediction, refrigeration, thermodynamics

INTRODUCTION

Refrigeration technology extensively utilizes lithium bromide (LiBr)-based brines as working fluids. Concentrated LiBr solutions have desirable properties as absorbents because of their high hydration heat, high solubility of solid phases, good thermal stability, and appropriate viscosity.[1] However, LiBr solutions can cause significant corrosion of construction materials.[2-4] In particular, corrosion problems are exacerbated by the recent trend toward using triple-effect technology, which involves the use of higher temperatures and more corrosive salts in addition to LiBr.[1] An important, practical problem associated with corrosion is the evolution of hydrogen, which impairs the efficiency of cooling cycles if preventive measures are not taken. Hydrogen evolution is a direct result of general corrosion of steel. Thus, it is necessary to use protection techniques such as pH control and application of inhibitors or inorganic coatings to minimize general corrosion.

The rate of corrosion in refrigeration cycles is determined by a multitude of factors such as temperature, concentration of the working fluid, pH, the presence of additional components, flow conditions, and metallurgical factors. Thus, it is desirable to develop a model that would reproduce the effect of these factors on corrosion rates, and as a result, save the cost of performing numerous experiments.

Working fluids frequently are multicomponent systems that include pH-adjusting agents and inhibitors. Therefore, it is desirable to incorporate the full chemistry of working fluids into the model. For this purpose, it is evident that the model should include thermophysical and electrochemical modules. The thermophysical module should predict the full speciation, activities of all species, and phase equilibria in the system. Additionally, the module should include transport properties (i.e., diffusivity and viscosity) that are necessary for the computation of

Submitted for publication September 1999.
* OLI Systems Inc., 108 American Road, Morris Plains, NJ 07950.

0010-9312/00/000105/$5.00+$0.50/0

flow effects on corrosion. The electrochemical module should predict surface processes that lead to corrosion as a function of solution chemistry, flow conditions, and metal characteristics.

Thus, the objective of this work was to develop a model that:

— Utilizes a comprehensive thermodynamic model to compute activities of species that participate in corrosion processes;

— Includes the partial cathodic and anodic processes that are responsible for general corrosion;

— Incorporates the effect of adsorption of halide ions on cathodic and anodic processes;

— Represents the active-passive transition and the effect of active ions on passivity;

— Reproduces observed corrosion rates using a reasonable set of physically meaningful parameters; and

— Reproduces the effect of pH control and selected inorganic inhibitors on corrosion rates.

THERMOPHYSICAL MODULE

The starting point for corrosion analysis is the computation of speciation in the investigated system. For this purpose, a thermodynamic model of electrolyte systems was used. This model combines information about standard-state properties of all species of interest with a formulation for the excess Gibbs energy, which accounts for solution nonideality. The model has been described in detail by Zemaitis, et al.,[5] and Rafal, et al.,[6] Its essential elements are summarized in Appendix A.

The thermodynamic model is used to predict concentrations and activities of ionic and neutral species in multicomponent systems that may contain an aqueous phase, any number of solid phases, and if necessary, a vapor and a nonaqueous liquid phase. Activities of individual species are used further in the electrochemical model. After completing speciation calculations, the thermophysical module computes the viscosity of the solution and diffusivities of all species using previously developed models.[7-8]

ELECTROCHEMICAL MODULE

The electrochemical model takes into account reactions on the surface of the metal and transport processes for species that participate in the reactions. The model focuses on partial cathodic and anodic processes that are expected to be important in systems containing concentrated brines, especially at elevated temperatures. The model takes into account halide adsorption and passivation phenomena, which may be influenced by pH control and inorganic inhibitors. Further, the model combines partial processes to compute corrosion rates in the framework of the mixed potential theory.

Electrochemical Reactions in the Absence of Halides

The mechanism of anodic dissolution of iron has been investigated extensively in acidic solutions.[9] While several variations of this mechanism have been proposed, the dependence of the dissolution rate on the activity of OH^- generally is accepted. The mechanism proposed by Bockris, et al.:[10]

$$Fe + OH^- \rightarrow FeOH_{ads} + e^- \quad (1)$$

$$FeOH_{ads} \rightarrow FeOH^+_{ads} + e^- \ (RD) \quad (2)$$

$$FeOH^+_{ads} \rightarrow Fe^{2+} + OH^- \quad (3)$$

predicts that the reaction order with respect to OH^- is 1. The validity of this prediction has been verified for acidic solutions.[10-11] Additionally, the current density for iron dissolution depends on the activity of water.[12] The mechanism of Bockris, et al., also predicts that the anodic transfer coefficient is 1.5.[10] Thus, the current density for iron dissolution is given by:

$$i_{Fe} = i^0_{Fe} \exp\left[\frac{\alpha_{Fe} F\left(E - E^0_{Fe}\right)}{RT}\right] \quad (4)$$

where i^0_{Fe} is the exchange current density, α_{Fe} = 1.5, and E^0 is the reversible potential of iron dissolution. The exchange current density can be expressed as:

$$i^0_{Fe} = i^*_{Fe} a_{OH} a^c_{H_2O} \quad (5)$$

where c is a reaction order with respect to the activity of water. According to Smart and Bockris, c = 1.6.[12] The effect of the activity of water on current density is significant for concentrated solutions, for which the activity of water usually is significantly different from one.

Although the reaction order with respect to OH^- is valid for acidic solutions, it has been found that iron dissolution proceeds with little influence of pH for solutions with pH > ≈ 4. Bockris, et al., explained this phenomenon by assuming a certain nonzero reaction order with respect to Fe^{2+} and considering the hydrolysis of Fe^{2+} that results from the dissolution.[10] Alternatively, the change in the reaction order with respect to OH^- can be reproduced by assuming that the exchange current density is proportional to the surface coverage by OH^-. This assumption is consistent with the reaction mechanism (Equation [1]). Thus, Equation (5) can be modified as:

$$i^0_{Fe} = i^*_{Fe} \theta_{OH} a^c_{H_2O} \quad (6)$$

Assuming that θ_{OH} follows the Langmuir adsorption model, Equation (6) can be rewritten as:

$$i^0_{Fe} = i^*_{Fe}\frac{a_{OH}}{1+K_{OH}a_{OH}}a^c_{H_2O} \quad (7)$$

It should be noted that Equation (7) reduces to Equation (5) for low activities of OH^- (i.e., for acidic solutions). For higher concentrations of OH^-, the reaction order with respect to OH^- becomes zero.

The reversible potential is calculated from the Nernst equation and depends upon Fe^{2+} activity. Additionally, a relationship is utilized that exists between the reversible potential and the exchange current density for anodic dissolution:[13-14]

$$\frac{RT}{\alpha_{Fe}F}\ln\frac{i^0_{Fe}}{i^{0\,\prime}_{Fe}} = E^0_{Fe} - E^{0\,\prime}_{Fe} \quad (8)$$

Equation (8) makes it possible to compute the exchange current density for any concentration of ferrous ions once it is established for a given Fe^{2+} concentration. The final expression for the anodic current density in the absence of halide ions is a combination of Equations (4), (7), and (8).

In general, cathodic processes may be caused by the reduction of H^+ or water molecules unless additional reducible species (such as oxygen) are present in the solution. In acidic solutions, the reduction of H^+ is the dominant cathodic reaction:

$$H^+ + e^- \rightarrow 0.5H_2 \quad (9)$$

Generally, it is accepted that the H^+ reduction reaction may proceed under activation or mass transfer control.[15] According to basic electrochemical kinetics,[15] the current density for H^+ reduction is:

$$\frac{1}{i_H} = \frac{1}{i_{H,a}} + \frac{1}{i_{H,lim}} \quad (10)$$

where $i_{H,a}$ and $i_{H,lim}$ are the activation and limiting current densities, respectively. The activation current density for proton reduction is:

$$i_{H,a} = i^0_H \exp\left[\frac{-\alpha_H F\left(E - E^0_H\right)}{RT}\right] \quad (11)$$

where α_H= 0.5[10] and E^0_H is calculated from the Nernst equation using previously calculated activities of H^+ and elemental hydrogen. The exchange current density is given by:

$$i^0_H = i^*_H a^{0.5}_H a^{2.2}_{H_2O} \quad (12)$$

In Equation (12), reaction orders, with respect to the activities of H^+ and H_2O, have been obtained from the studies of Bockris, et al.,[10] and Smart and Bockris,[12] respectively.

The limiting current density in Equation (10) results from diffusion-limited transport of protons to the metal surface and can be calculated as:

$$i_{H,lim} = k_m F a_H \quad (13)$$

where k_m is the mass transfer coefficient. The value of k_m can be calculated if the flow regime, diffusion coefficient of H^+, and solution viscosity are known. Formulas for the computation of k_m are discussed in Appendix B.

As the pH of a solution increases, the importance of the proton reduction reaction rapidly decreases. In neutral and alkaline solutions, the predominant reaction is the reduction of water molecules:

$$H_2O + e^- \rightarrow 0.5H_2 + OH^- \quad (14)$$

Unlike the reduction of protons, the water reduction does not exhibit a limiting current density because there are no diffusion limitations for the transport of H_2O molecules to the surface. Thus, the current density can be expressed as:

$$i_{H_2O} = i^0_{H_2O}\exp\left[\frac{-\alpha_{H_2O}F\left(E - E^0_H\right)}{RT}\right] \quad (15)$$

As in the case of proton reduction, α_{H_2O} = 0.5. The reversible potential in Equation (15) is the same as in Equation (11) because the reduction of water is thermodynamically equivalent to the reduction of protons. The reaction order with respect to water activity can be assumed to be the same as that for proton reduction. Thus, the exchange current density is given by:

$$i^0_{H_2O} = i^*_{H_2O}a^{-0.5}_H a^{2.2}_{H_2O} \quad (16)$$

For all partial processes, the concentration-independent part of the exchange current density (i.e., i^*) is assumed to be temperature dependent by introducing a nonzero enthalpy of activation:

$$i^*(T) = i^*(T_{ref})\exp\left[-\frac{\Delta H}{R}\left(\frac{1}{T} - \frac{1}{T_{ref}}\right)\right] \quad (17)$$

Effect of Halide Adsorption

Adsorption of halide ions on iron and carbon steels has been studied extensively by several investigators.[16-26] In particular, it has been determined that

adsorption of halide ions can be reproduced quantitatively using the Frumkin isotherm.[24] This indicates that chemisorption occurs. Halide ions act as good ligands for iron because they exhibit a low electronegativity. Among the halide ions, polarizability increases in the order $Cl^- < Br^- < I^-$, which coincides with the increase in the ionic radius. Thus, the tendency for adsorption also should increase in this order. This is in agreement with experimental observations that the adsorption coverage in relatively dilute solutions increases in the order $Cl^- < Br^- < I^-$. Thus, at relatively low or moderate halide concentrations, adsorption of halides leads to a reduction in corrosion rates. However, the effect of halides is not limited to blocking the surface through adsorption. Adsorbed halide ions also can interfere with the mechanism of anodic dissolution of iron, which may lead to an increase in the corrosion rate at higher concentrations of halide ions.

For the quantitative representation of the effect of adsorption, the requirement that the rate of adsorption should be equal to the rate of desorption in the stationary state should be the first step:

$$v_{ads,i} = v_{des,i} \tag{18}$$

where i denotes any adsorbable species. At the conditions for which halide adsorption does not interfere with the metal dissolution, the rates can be expressed using the Frumkin isotherm:

$$v_{ads,i} = k_{ai}\left(1-\sum_j \theta_j\right)a_i \exp\left(-\beta\sum_j A_{ij}\theta_j\right) \tag{19}$$

$$v_{des,i} = k_{di}\theta_i \exp\left[(1-\beta)\sum_j A_{ij}\theta_j\right] \tag{20}$$

where the transfer coefficient (β) commonly is assumed to be equal to 0.5, a_i is the activity of species i in the bulk solution, A_{ij} is the Frumkin interaction coefficient, and k_{ai} and k_{di} are the adsorption and desorption rate constants, respectively.

Combination of the expressions for the adsorption and desorption rates yields the Frumkin isotherm in a version for multicomponent systems:[16]

$$\frac{k_{ai}}{k_{di}}a_i = \frac{\theta_i}{1-\sum_j \theta_j}\exp\left(\sum_j A_{ij}\theta_j\right) \tag{21}$$

In Equation (21), the k_{ai} and k_{di} constants are not independently measurable, and only their ratio can be established.

Equation (21) is valid only when adsorption is not influenced significantly by metal dissolution. To include the effect of dissolution, Heusler and Cartledge proposed an additional process in which a metal atom from an uncovered $(1 - \sum\theta_j)$ area reacts with a hydroxyl ion and an adsorbed halide ion from the covered area θ_i to dissolve as ferrous ion.[19] The adsorbed halide was postulated to leave the surface during the reaction, thus contributing to the desorption process. This mechanism was confirmed by matching calculated and measured polarization curves.[19] To include the effect of dissolution-related desorption, Equation (20) can be rewritten by adding an additional term:

$$v_{des,i} = k_{di}\theta_i \exp\left[(1-\beta)\sum_j A_{ij}\theta_j\right] + i_{des,i} \tag{22}$$

where the desorption current ($i_{des,i}$) is given by:

$$i_{des,i} = k_{ri}\theta_i\left(1-\sum_j \theta_j\right)a_{OH}\exp\left(\frac{2\beta FE}{RT}\right) \tag{23}$$

In Equation (23), the desorption current is potential dependent because it involves the dissolution of the metal. In view of the proposed mechanism, it is proportional to the halide coverage fraction (θ_i) and the uncovered area $(1 - \sum\theta_j)$. Equation (23) can be combined with Equations (19) and (22) to form a system of n nonlinear equations for a solution with n adsorbable species. This system can be solved numerically for the coverage fractions (θ_i) of each adsorbed species. Because of the potential dependence, the model predicts that the adsorption coverage rapidly decreases above a certain potential range, which depends primarily on the activity of halide ions and OH^-.

The three reaction rate constants (k_{ai}, k_{di}, and k_{ri}) are not independent and only the ratios k_{di}/k_{ai} and k_{ri}/k_{ai} can be determined. Thus, the adsorption model described above is characterized by k_{di}/k_{ai}, k_{ri}/k_{ai}, and A_{ij} as parameters. These parameters have been obtained by analyzing experimental polarization and, secondarily, corrosion rate data for varying concentrations of halide ions.[18,21-22,24-26]

Halide-Accelerated Dissolution

In concentrated solutions, adsorbed halide ions may accelerate the dissolution of iron or carbon steel. A number of reaction mechanisms have been proposed to explain this phenomenon. In particular, Nobe and coworkers developed a mechanism that postulates a reaction route that is parallel to Equations (1) through (3).[21-22] An essentially identical mechanism also has been proposed by Drazic and Drazic.[25] According to this mechanism, a halide-containing surface complex is responsible for the

dissolution. Thus, Equation (1) is followed by the following parallel route:

$$FeOH_{ads} + X^- \rightarrow FeOHX^-_{ads} \quad (24)$$

$$FeOHX^-_{ads} \rightarrow FeOHX_{ads} + e^- \quad (RD) \quad (25)$$

$$FeOHX_{ads} + H^+ \rightarrow Fe^{2+} + X^- + H_2O \quad (26)$$

The mechanism in Equations (24) through (26) results in a dissolution current density that depends upon the activities of halide ions and OH^-:

$$i_{Fe,X_k} = i^*_{Fe,X_k} a^s_{X_k^-} a^t_{OH^-} \exp\left[\frac{F\left(E - E^0_{Fe}\right)}{RT}\right] \quad (27)$$

where k denotes various halide ions that may be present in the system.

For chloride systems, Kuo and Nobe found that s = 0.4 and t = 0.6 when concentrations are used instead of activities.[22] For bromide systems, the reaction orders determined in this study are s = 1 and t = 3. Since the mechanism described by Equations (24) through (26) is assumed to be parallel to the mechanism under halide-free conditions, the total current density of anodic dissolution can be assumed to be a sum of the contributions of two mechanisms. Additionally, the desorption current density contributes to the total current (Equation [23]), although it becomes important only at relatively high potentials and its numerical significance usually is limited. Thus, the expression for the total current becomes:

$$i_{Fe}' = i_{Fe} + \sum_k i_{Fe,X_k} + \sum_j i_{des,j} \quad (28)$$

Active-Passive Transition

Corrosion control strategies for adsorption refrigeration systems rely on the use of inhibitors at high temperatures to influence passivity. Thus, it is necessary to introduce the active-passive transition into the expression for the anodic current density. For this purpose, a convenient method has been proposed.[27] According to the approach of Ebersbach, et al.,[27] the current that leads to the formation of a passive layer is considered separately from the current that leads to active dissolution. At any instant, a certain fraction of the surface (θ_p) is assumed to be covered by the passive layer. The change of the passive layer coverage fraction with time can be expressed as:

$$\left(\frac{\partial \theta_P}{\partial t}\right)_{E,a_i} = ci_2(1 - \theta_P) - K\theta_P \quad (29)$$

where i_2 is the current density that contributes to the formation of a passive layer. The second term on the right-hand side of Equation (29) represents the rate of dissolution of the passive layer, which is proportional to the coverage fraction. c and K are proportionality constants. The total current density is expressed as:

$$i_{Fe,TOT} = \left(i_{Fe}' + i_2\right)\left(1 - \theta_p\right) \quad (30)$$

where i_{Fe}' is the current density for active dissolution of iron. Equation (29) can be solved with respect to θ_p, and the result can be substituted into Equation (30). In the stationary state ($t \rightarrow \infty$), the total anodic current becomes:

$$i_{Fe,TOT} = \frac{i_{Fe}' + i_2}{1 + \frac{ci_2}{K}} = \frac{i_{Fe}' + i_2}{1 + \frac{i_2}{i_p}} \quad (31)$$

In Equation (31), the c/K ratio constitutes the passive current density. i_2 can be represented by the usual expression for processes under activation control:

$$i_2 = i_2^0 \exp\left[\frac{\alpha_2 F(E - E_F)}{RT}\right] \quad (32)$$

Thus, in addition to the passive current density, the model of the active-passive transition is characterized by two parameters (i.e., i_2^0 and α_2). These are determined based on observable characteristics of the active-passive transition, such as the Flade potential and the critical current density.[15,28-31]

Effect of Solution Chemistry on Passivity

In the absence of active ions, the passive current density depends primarily on the pH of the solution.[15] Halide ions cause the breakdown of passive films, which manifests itself as an increase in the passive current in addition to the onset of localized corrosion.[32] However, corrosion inhibitors such as molybdates or chromates may repair passive films, thus reducing the passive current density. In this study, there was no concern for localized corrosion and only the effect of halide ions on the magnitude of the passive current density was examined.

As shown by Vetter,[15] the pH dependence of the corrosion current density (I_{corr}) in the passive state is determined by a reaction between O^{2-} in the passive oxide layer and protons from the solution. In acidic solution, this dissolution reaction can be written as:

$$\equiv FeO_a(OH)_b + sH^+ = Fe(OH)_g^{t+} \quad (33)$$

where ≡ denotes the solid substrate and the formula ≡ $FeO_a(OH)_b$ represents the stoichiometry of the hydrated oxide in the passive layer. In general, the hydrated oxide is subject to compositional variations, and the stoichiometry of Reaction (33) may vary. Reaction (33) leads to a linear dependence of the passive current density on pH, which is in agreement with experimental data in acidic solutions.[33] For neutral and alkaline solutions, Reaction (33) can be modified as:

$$\equiv FeO_a(OH)_b + uH_2O = Fe(OH)_3^0 \qquad (34)$$

Reactions (33) and (34) lead to an expression for the passive current density as a function of proton and water activity:

$$i_p = k_H a_{H^+}^s + k_{H_2O} a_{H_2O}^u \qquad (35)$$

Equation (35) predicts a linear pH dependence of i_p in acidic solutions and a pH-independent value for nearly neutral or alkaline solutions. This behavior agrees with experimental results.[15,28,33]

To analyze the effect of active ions on the passive current density, surface reactions were considered between the passive oxide layer and the i-th ion from the solution:

$$\equiv FeO_aOH_b + c_iX_i = \equiv FeO_{di}(OH)_{fi}X_{ci} + e_iOH^- \qquad (36)$$

In Equation (36), the stoichiometry is usually difficult to define because of the dynamic nature of the system and may be, in general, fractional. It is reasonable to assume that Equation (36) is in quasi equilibrium.[34] Therefore, it may be characterized by an equilibrium constant:

$$K_i = \frac{N_i a_{OH^-}^{e_i}}{\left(N_0 - \sum_k N_k\right) a_{X_i}^{c_i}} \qquad i = 1,\ldots n \qquad (37)$$

where i pertains to the i-th active ion, N_i is the number of sites per surface unit that are occupied by complexes containing the i-th active ion, and N_0 is the total number of sites per surface area. Equation (37) describes a system of equations that represent surface reactions involving any number of active species. This system may be solved with respect to N_i:

$$N_i = \frac{N_0 K_i \dfrac{a_{X_i}^{c_i}}{a_{OH^-}^{e_i}}}{1 + \sum_k K_k \dfrac{a_{X_k}^{c_k}}{a_{OH^-}^{e_k}}} \qquad (38)$$

The surface Reaction (36) is followed by a dissolution reaction. The surface species that forms as a result of Reaction (36) may undergo dissolution reactions that are analogous to Reactions (33) or (34):

$$\equiv FeO_{di}(OH)_{fi}X_{ci} + sH^+ \rightarrow Fe(OH)_g^{f+} + c_iX_i \qquad (39)$$

and:

$$\equiv FeO_{di}(OH)_{fi}X_{ci} + uH_2O \rightarrow Fe(OH)_3^0 + c_iX_i \qquad (40)$$

On the right-hand side of Equations (39) or (40), the active anions may form further aqueous complexes with hydrolyzed iron cations.

In acidic solutions, the dissolution rate for sites occupied by complexes with active ions is given, according to Equation (39), by:

$$i_{p,i} = k_i N_i a_{H^+}^s \qquad (41)$$

whereas the dissolution rate for the free sites is:

$$i_{p,0} = k'_H\left(N_0 - \sum_k N_k\right) a_{H^+}^s \qquad (42)$$

The total current density in the passive state is the sum of Equations (41) and (42):

$$i_p = i_{p,0} + \sum_k i_{p,k} \qquad (43)$$

Analogous expressions can be written for the active species-assisted dissolution in neutral and alkaline solutions (Equations [40]). Assuming that the surface reactions (Equations [36]) are characterized by the same parameters over the whole pH range, the total passive current density can be expressed as:

$$i_p = \left(k_H a_{H^+}^s + k_{H_2O} a_{H_2O}^u\right) \frac{1 + \sum_i l_i \dfrac{a_{X_i}^{c_i}}{a_{OH^-}^{e_i}}}{1 + \sum_i K_i \dfrac{a_{X_i}^{c_i}}{a_{OH^-}^{e_i}}} \qquad (44)$$

where l_i is a composite parameter that contains the forward dissolution rate constant (k_i) and the quasi-equilibrium constant, K_i. In Equation (44), k_H and k_{H_2O} are determined using data for passive film dissolution in the absence of active ions.[15,29-30,33,35-38] In the case of halide ions, the l_i values are greater than the K_i values, which results in a significant increase in the passive current density. This reflects the fact that the surface reaction is followed by accelerated disso-

lution. At the same time, inhibitor ions are characterized by large K_i and small l_i values. Thus, according to the model, inhibitor ions are envisaged to form surface complexes that block reaction sites on the surface of the passive layer. In this case, the surface reaction is not followed by accelerated dissolution. Thus, the presence of inhibitor ions counteracts the effect of halide ions and limits the current density. In this way, the model simultaneously takes into account the ions that promote the dissolution of the passive film ($K_i < l_i$) and those that inhibit the dissolution ($K_i >> l_i$).

Implementation of the Model

Parameters of the electrochemical model have been determined by utilizing a large number of experimental polarization and corrosion rate data. To ensure the validity of the model under a substantial range of conditions, these data were not limited to corrosion in LiBr-based systems. In particular, the parameters for the proton reduction, water reduction, and iron oxidation processes were determined from data on the corrosion of iron and mild steel in various mineral acids, bases, and saline solutions.[39-40] Corrosion data for LiBr + H_2O were utilized only for establishing parameters of processes specific to LiBr corrosion (e.g., the bromide-assisted anodic dissolution).

The model described above has been implemented in a program for the prediction and analysis of corrosion rates. As input, the program accepts the composition of corrosive medium, temperature, and pressure. Then, thermodynamic calculations are performed to compute the speciation of the system and predict stable phases. Depending on conditions, the system may be made up of an aqueous phase that includes electrolyte components, a gas phase, and any number of solid phases. Thermodynamic calculations (Appendix A) make it possible to obtain concentrations and activities of individual species, which are used further as input for the electrochemical model. Additionally, the program returns diffusivities of individual species and the viscosity of the aqueous phase.

To execute the electrochemical model, the program requires flow conditions as additional input (Appendix B). Then, the program computes the current density — potential relationships for individual cathodic and anodic processes. Further, individual processes are combined into a total predicted polarization curve. The corrosion potential (E_{corr}) is calculated by applying the mixed-potential theory:

$$\sum i_{c,i} = \sum i_{a,j} \qquad (45)$$

where $i_{c,i}$ and $i_{a,j}$ denote the i-th cathodic and j-th anodic process. Once E_{corr} is obtained by solving Equation (45), I_{corr} also is computed.

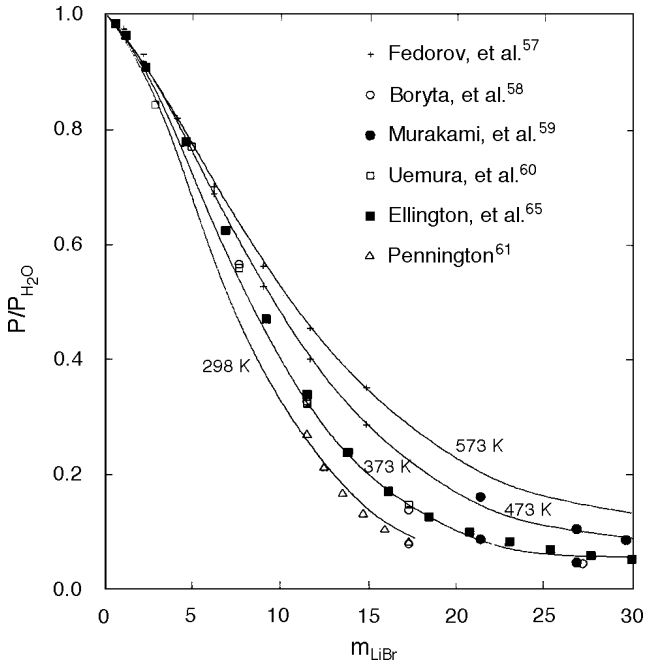

FIGURE 1. *Saturated vapor pressures of aqueous LiBr solutions as a function of LiBr molality at various temperatures. The lines were obtained from the thermodynamic model and the symbols represent literature data.*[57-61,65]

RESULTS AND DISCUSSION

The thermodynamic model was verified using experimental vapor pressure and solubility data for LiBr-based systems. Figure 1 shows results of vapor pressure calculations for the LiBr + H_2O solution in wide concentration ranges at temperatures to 573 K. Very good agreement with experimental data from various sources was obtained. Similarly, Figure 2 shows a solubility diagram for LiBr + H_2O, which is characterized by the presence of four separate hydrates as solid phases. The model represents the data within experimental uncertainty. Results of thermodynamic calculations for more complex absorption cooling systems have been reported in a separate study.[41] The agreement with experimental vapor pressure and solubility data indicates that the model correctly reproduces activities of solution species. Thus, activities can be used with confidence in the electrochemical model.

After validating the thermodynamic module, the electrochemical model was applied first to systems that clearly showed the effect of halide adsorption on corrosion rates. To verify the effect of adsorption, it was convenient to analyze corrosion rates with respect to changing concentrations of halide ions. Such analysis is shown in Figure 3 for a mixture containing sulfuric acid (H_2SO_4), sodium sulfate (Na_2SO_4), and increasing amounts of potassium chloride (KCl), and another mixture containing hydrochloric acid

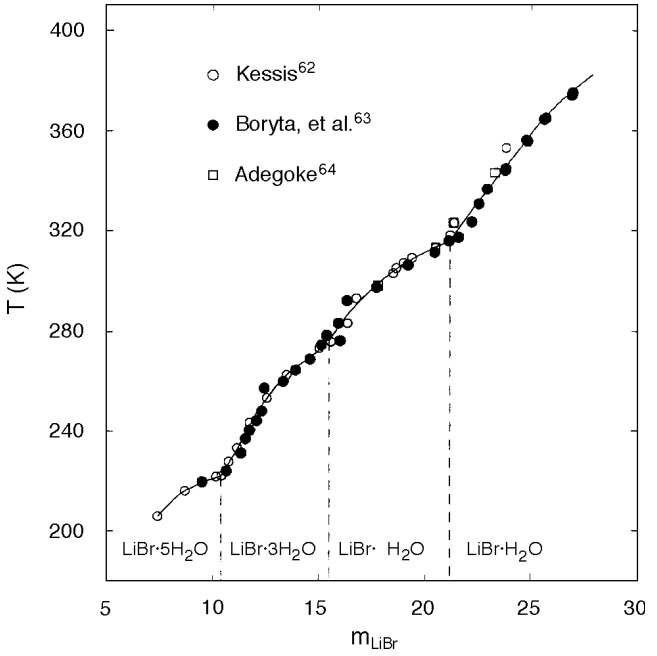

FIGURE 2. *Solubility of various hydrates of solid phases in aqueous LiBr solutions. The lines were calculated from the thermodynamic model and the symbols represent literature data.[62-64]*

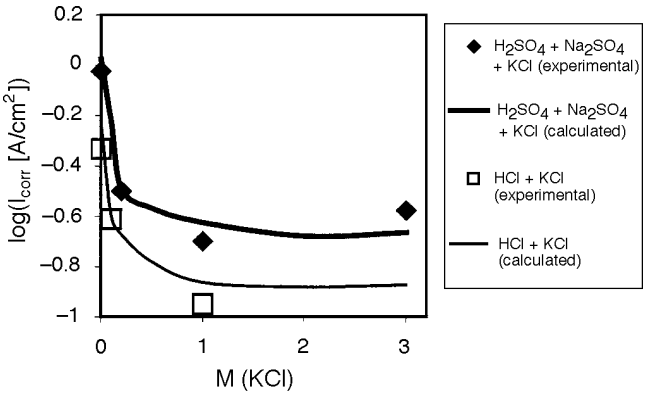

FIGURE 3. *Effect of Cl^- concentration on the corrosion current for iron in H_2SO_4 + Na_2SO_4 + KCl and HCl + KCl solutions at 25° C. The lines were calculated from the model and the symbols represent literature data.[18]*

(HCl) and increasing amounts of KCl. Since the halide concentrations shown in Figure 3 were moderate (up to 3 M), adsorption resulted primarily in a reduction of corrosion rates. Calculated results were in good agreement with the data of Schwabe and Voigt.[18] The decrease in corrosion rates was observed primarily for dilute solutions and the rates appeared to stabilize at higher concentrations. This was also in agreement with results of Jesionek and Szklarska-Smialowska,[24] who have shown that substantial surface coverages are obtained for relatively dilute halide solutions.

In addition to halide ion concentrations, pH is an important independent variable. To verify the accuracy of computation of pH effects using the electrochemical model, calculations were performed for the corrosion of iron in systems with a fixed amount of halide ions and varying pH. In such a system, the effect of halide adsorption is constant, whereas the corrosion rate depends primarily on the activity of H^+. Results are shown in Figure 4 for 1-M solutions of hydrogen bromide (HBr) and potassium bromide (KBr) with varying pH.[32] As shown in Figure 4, the pH effect on I_{corr} was reproduced with good accuracy. In addition to I_{corr}, Figure 4 shows that the model reproduced experimental values of E_{corr}. Simultaneous representation of E_{corr} and I_{corr} indicated that the model accurately captured the balance between

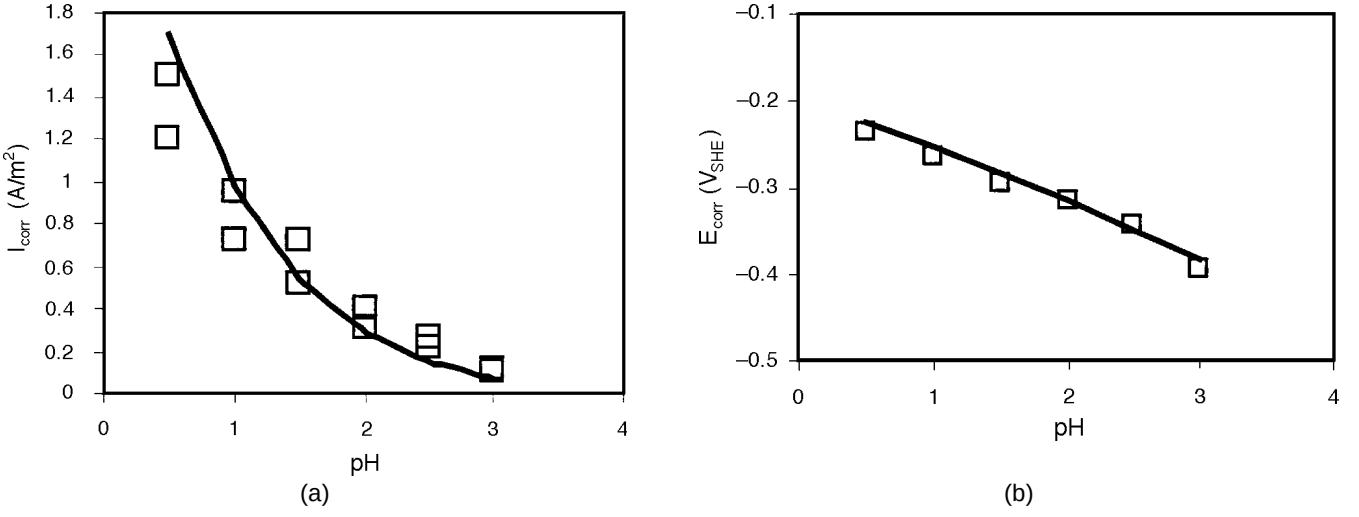

FIGURE 4. *I_{corr} and E_{corr} of iron in a 1-M solution of HBr and KBr of varying acidity. The lines were obtained from the model and the symbols represent literature data.[32]*

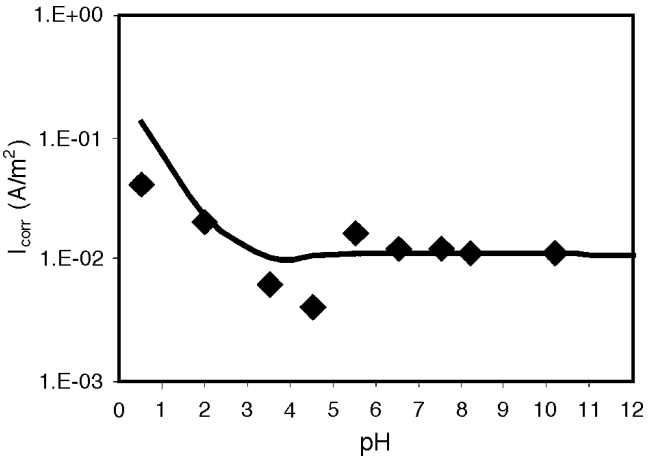

FIGURE 5. *I_{corr} as a function of pH for carbon steel in a 4.6-M LiBr solution at 25°C. The line was calculated from the model and the symbols denote literature data.[2]*

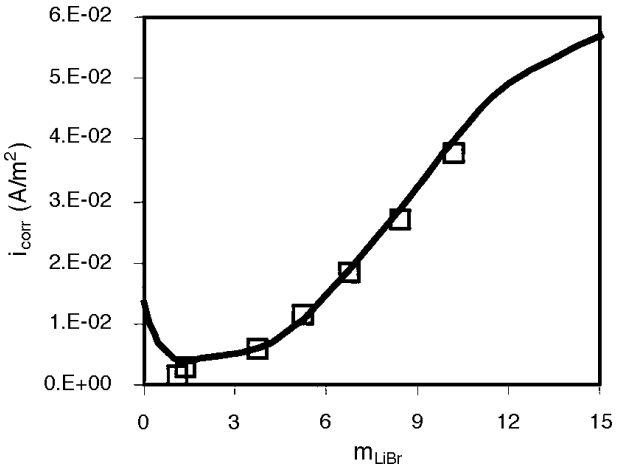

FIGURE 6. *Corrosion rates for carbon steel in LiBr solutions of varying concentrations at 25°C. The lines were obtained from the model and the symbols denote literature data.[2]*

the iron oxidation and proton reduction reactions, which depended upon proton activity in different ways (Equations [5] and [12]).

Figure 5 shows the computed I_{corr} for carbon steel in a 4.6-M LiBr solution in a wider pH range. Because of moderate temperature, I_{corr} was low in neutral and weakly acidic solutions. The model represents the data essentially within experimental scattering.[2]

As the activity of halide ions increased to high values, the corrosion rate increased because of halide-assisted dissolution (Equations [24] through [28]). For LiBr solutions, this was observed for concentrations > 3 m to 4 m. This behavior is illustrated in Figure 6 for the LiBr-H_2O system at 25°C. The increase in corrosion rate with increasing Br concentrations in near-neutral solutions was very significant, although the slope of the rate vs LiBr molality curve somewhat decreased at very high concentrations. This is a general phenomenon that persists at higher temperatures. As shown in Figure 6, the model predictions agreed with the data of Guiñon, et al.[2]

After verifying the model for systems at room temperature, calculations were performed for elevated temperatures, which are of primary interest for absorption cooling cycles. In this case, the model was validated primarily against the data of Tanno and coworkers.[3,42] At elevated temperatures, the experimental corrosion rates were inherently much more uncertain. This is illustrated in Figure 7 for LiBr + H_2O at temperatures ranging from 100°C to 160°C and at three concentrations. The data showed significant scattering, especially at the highest concentration (23 M). As with corrosion rates at low temperatures, a significant increase in corrosiveness was observed with increased concentration. The

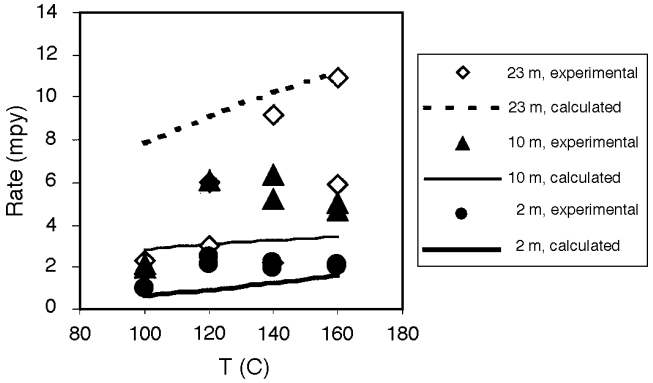

FIGURE 7. *Corrosion rates of carbon steel in LiBr solutions at temperatures ranging from 100°C to 160°C and concentrations ranging from 2 m to 23 m. The experimental data were obtained by Tanno, et al.,[3] and the lines were obtained from the model.*

model was consistent with the data, and computed corrosion rates were within the limits of experimental uncertainty. The model predicted that corrosion rates increased with temperature, but the slope of the rate vs temperature curves was relatively small.

The simplest corrosion control method is the alkalization of the working fluid using lithium hydroxide (LiOH). It is well known that the presence of OH^- influences the passivity of steels. However, the effectiveness of this approach is limited. The electrochemical model can be used to simulate the effect of hydroxide addition and the limits of its usefulness. As shown by Equation (44), the passive current density is a function of activities of ions that promote the dissolution of passive films, such as Br^-. At the same time, the passive current density depends upon the activity of OH^-, which plays a role in the dissolution reaction (Equation [44]). In general, an increase in

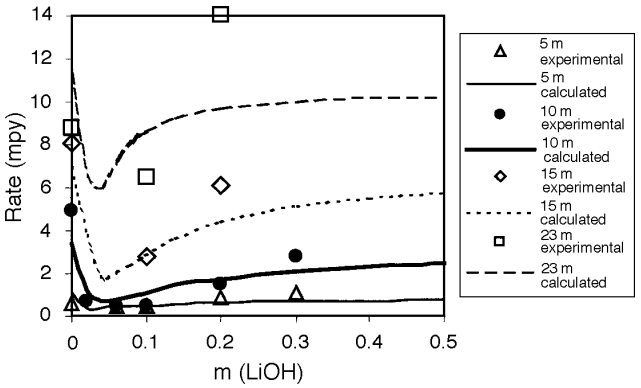

FIGURE 8. *Corrosion rate as a function of LiOH molality for carbon steel at 160°C in LiBr solutions with various concentrations. The experimental data (symbols) were obtained by Tanno, et al.[42]*

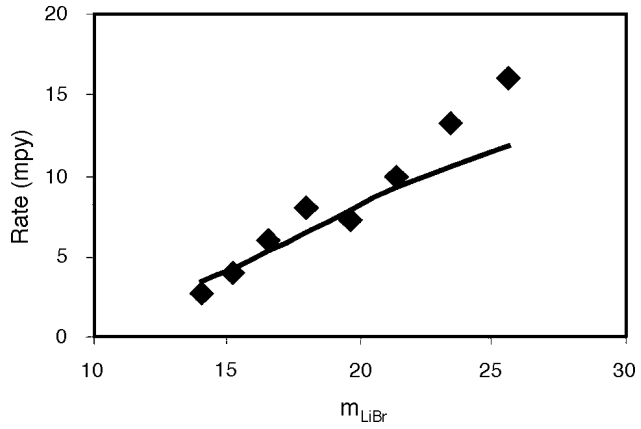

FIGURE 9. *Corrosion rate of carbon steel in LiBr solutions of varying concentration at the normal boiling temperature (i.e., from 138.3°C at 14.07 m to 185.3°C at 25.63 m). Solutions were inhibited with 0.2 wt% LiOH. The line was calculated from the model and the symbols represent the literature data.[43]*

OH^- concentration may reduce the passive current density. However, the interplay between the Br^- and OH^- leads to a complex behavior of corrosion rates.

For the LiBr + LiOH system, the calculated corrosion rates were compared with experimental data of Tanno, et al.[42] Figure 8 shows the predicted corrosion rate as a function of LiOH molality for carbon steel at 160°C. In the case of LiBr solutions with relatively low and moderate concentrations (i.e., 5, 7.5, and 10 M), the corrosion rate was reduced significantly by the presence of LiOH. In this case, corrosion rates < 1 mpy were obtained. The concentration of LiOH necessary for the reduction of corrosion rates depends upon the LiBr concentration and is predicted to vary from ≈ 0.02 M to 0.05 M. Although the data showed a significant degree of scattering (Figure 8), no systematic deviations were observed between the calculated results and experimental data.[42]

The effect of LiOH on corrosion rates became much less significant when the LiBr concentration was high (23 M in Figure 8). In this case, the model predicted only a small dip in corrosion rate as a function of LiOH molality, and the corrosion rates remained fairly high in the entire range of LiOH concentrations. In this case, the activity of Br^- was so high that it practically overwhelmed the effect of OH^-.

Additionally, Figure 9 shows corrosion rates of carbon steel in LiBr solutions of varying concentrations at the normal boiling temperature (i.e., from 138.3°C at 14.07 M to 185.3°C at 25.63 M). All solutions contained 0.2 wt% LiOH. Thus, these calculations represented the combined effect of temperature and LiBr concentration on the corrosion rate. As shown in Figure 9, the calculated results were consistent with the data of Dockus, et al.[43] This result was especially noteworthy in view of the fact that different carbon steel specimens were used in the experiments of Tanno, et al.,[42] and Dockus, et al.[43] This indicates that metallurgical factors did not affect strongly the rates of uniform corrosion of carbon steel in LiBr + LiOH systems.

An important practical problem in the control of corrosion in absorption cooling cycles is the selection of inhibitors. Results showed that pH control was effective for reducing corrosion rates when the concentration of LiBr was not very high. In such cases, corrosion rates < 1 mpy were obtained. For very concentrated LiBr solutions, it was necessary to use additional inhibitors to reduce the rate to an acceptable level. In this study, the inhibiting effect of molybdates and chromates was analyzed.

Molybdates generally are known to reduce the passive current density.[44-46] Under typical conditions at low or moderate temperatures, it is necessary to use molybdates in conjunction with selected oxidizing agents (e.g., dissolved oxygen or nitrites) to increase the potential and, in this way, shift the mixed potential to the passive region.[46] However, the use of additional oxidizing agents does not seem to be necessary at elevated temperatures that are of interest for absorption cooling cycles. In this case, a reduction in the passive current density may be sufficient to reduce corrosion rates. Thus, molybdates can be expected to reinforce the effect of OH^-, which are capable of reducing corrosion for LiBr solutions up to moderate concentrations.

Parameters that represent the effect of molybdate ions on passive current density (Equation [44]) have been calibrated using experimental polarization data at room temperature.[44] After determining the parameters, the model was applied to LiBr-based systems. Figure 10 shows the effect of molybdate ions on the corrosion rates in solutions containing 0.1 M LiOH and two concentrations of LiBr (i.e., 10 M or 23 M). In the case of solutions with moderate concentrations of LiBr (10 M), the corrosion rate was already low in the absence of molybdates. This was caused by the passivating effect of OH^-. In this case,

the addition of lithium molybdate (Li_2MoO_4) resulted in only marginal reduction of corrosiveness. However, the effect of Li_2MoO_4 was very significant for high concentrations of LiBr (i.e., 23 M). In this case, OH^- was insufficient to induce passivation. However, a small amount of molybdate ions (i.e., ≈ 0.002 M) reduced the corrosion rate to a low value (~ 1 mpy). Results of computations were in agreement with the experimental data of Tanno, et al.[42] (Figure 10). In Figure 11, the effect of molybdates is compared with experimental data obtained for a different carbon steel specimen.[47] In this case, corrosion rates were computed for a 20.47-M LiBr solution at 160°C with and without 0.24 M LiOH and 0.032 M Li_2MoO_4. The predicted values were consistent with experimental data in both cases.

Chromates also have been reported to be effective for the inhibition of corrosion in LiBr solutions.[48] The presence of chromates reinforces the passive film by the formation of mixed iron(III) and chromium(III) oxides.[49] Within the framework of the electrochemical model, this effect was reproduced using the model for interactions of solution species with passive films (Equations [36] through [44]).

The chromate-passive film interaction parameters of Equation (44) have been calibrated using the room-temperature data of Cohen and Jelinek.[48] As shown in Figure 12, the model accurately reproduced the inhibition of corrosion in a 13.52-M (54 wt%) LiBr + 0.18-M (0.2 wt%) LiOH solution.[48] With the obtained parameters, the model was applied to predict the behavior of chromates at high temperatures. In Figure 11, results are shown for the corrosion rate in a solution containing 0.0066 M LiOH and 0.058 M lithium chromate (Li_2CrO_4) at 160°C. In this case, chromate ions significantly reduced the corrosion rate, although they were slightly less effective than molybdates. The calculated results were in agreement with the experimental data at elevated temperatures.[47]

CONCLUSIONS

❖ A comprehensive model was developed for simulating the rates of general corrosion of carbon steels in LiBr-based working fluids, which are used in absorption refrigeration cycles.
❖ The model consists of a thermophysical module that provides comprehensive speciation calculations and an electrochemical module that predicts the partial reduction and oxidation processes on the surface of the metal.
❖ The model has been validated extensively using thermodynamic and corrosion rate data. Good agreement with experimental results was obtained.
❖ The model accurately represents the effect of pH control and selected inhibitors on corrosion rates. Thus, it can serve as a prediction tool for designing

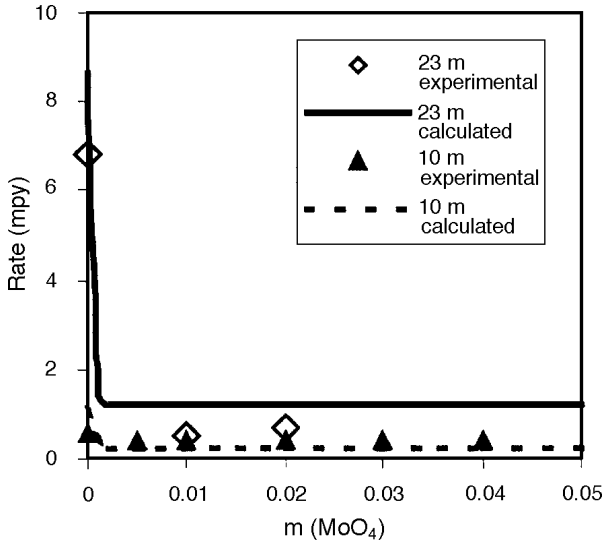

FIGURE 10. *Effect of molybdate ions on corrosion rates of mild steel in solutions containing 0.1 m LiOH and various concentrations of LiBr. The symbols denote literature data.[42]*

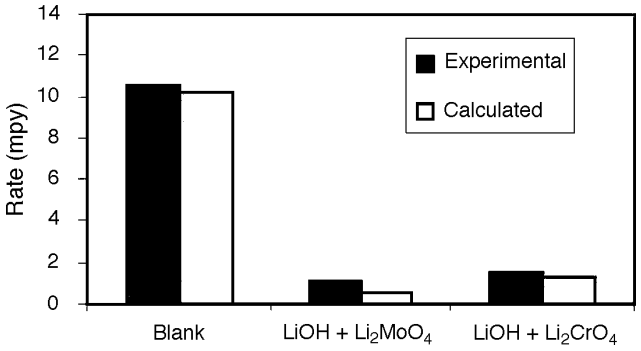

FIGURE 11. *Corrosion rates of carbon steel in uninhibited and inhibited 20.47 m LiBr solution at 160°C. The molybdate-inhibited solution contained 0.24 m LiOH and 0.032 m Li_2MoO_4, and the chromate-inhibited solution contained 0.0066 m LiOH and 0.058 m Li_2CrO_4. The solid bars denote literature data.[47]*

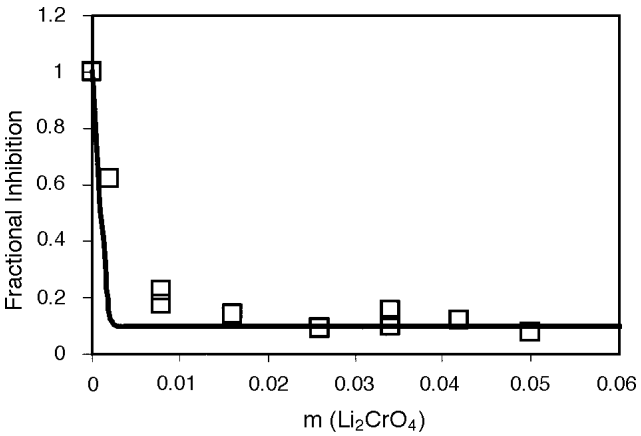

FIGURE 12. *Effect of chromate ions on the corrosion rate in 13.52 m (54 wt%) LiBr + 0.18 m (0.2 %) LiOH solution. The symbols denote literature data.[48]*

absorption refrigeration systems at conditions that have not been investigated experimentally.

ACKNOWLEDGMENTS

The authors acknowledge the financial support of the Gas Research Institute under contract number 5096-260-3 596 and the technical guidance provided by K. Krist. The authors also benefited from discussions with S. Kujak of the Trane Company.

REFERENCES

1. K.E. Herold, R. Radermacher, S.A. Klein, Absorption Chillers and Heat Pumps (Boca Raton, FL: CRC Press, 1996), p. 101.
2. J.L. Guiñon, J. Garcia-Anton, V. Perez-Herranz, G. Lacoste, Corrosion 50 (1994): p. 240.
3. K. Tanno, M. Itoh, T. Takahashi, H. Yashiro, N. Kumagai, Corros. Sci. 34 (1993): p. 1,441-1,451.
4. D. Itzhak, O. Elias, Corrosion 50 (1994): p. 131.
5. J.F. Zemaitis, Jr., D.M. Clark, M. Rafal, N.C. Scrivner, Handbook of Aqueous Electrolyte Thermodynamics (New York, NY: American Institute of Chemical Engineers [AIChE], 1986).
6. M. Rafal, J.W. Berthold, N.C. Scrivner, S.L. Grise, "Models for Electrolyte Solutions," in Models for Thermodynamic and Phase Equilibria Calculations, ed. S.I. Sandler (New York, NY: Marcel Dekker, 1995), p. 601.
7. M.M. Lencka, A. Anderko, S.J. Sanders, R.D. Young, Int. J. Thermophys. 19 (1998): p. 367.
8. A. Anderko, M.M. Lencka, Ind. Eng. Chem. Res. 37 (1998): p. 2,878.
9. D.M. Drazic, "Iron and Its Electrochemistry in an Active State," in Modern Aspects of Electrochemistry, no. 19, eds. B.E. Conway, J.O'M. Bockris, R.E. White (New York, NY: Plenum Press, 1989), p. 69.
10. J.O'M. Bockris, D. Drazic, A.R. Despic, Electrochim. Acta 4 (1961): p. 325.
11. E.J. Kelly, J. Electrochem. Soc. 112 (1965): p. 124.
12. N.G. Smart, J.O'M. Bockris, Corrosion 48 (1992): p. 277.
13. J.M. West, Electrodeposition and Corrosion Processes (New York, NY: Van Nostrand, 1964), p. 36.
14. S. Nesic, J. Postlethwaite, S. Olsen, Corrosion 52 (1996): p. 280.
15. K.J. Vetter, Electrochemical Kinetics (New York, NY: Academic Press, 1967), pp. 516, 755.
16. E. Gileadi, ed., Electrosorption (New York, NY: Plenum Press, 1967), p. 1.
17. M.A. Habib, J.O'M. Bockris, Comprehensive Treatise of Electrochemistry, vol. 1., eds. J.O'M. Bockris, B.E. Conway, E. Yeager (New York, NY: Plenum Press, 1980), p. 135.
18. K. Schwabe, C. Voigt, Electrochim. Acta 14 (1969): p. 853.
19. K.E. Heusler, G.H. Cartledge, J. Electrochem. Soc. 108 (1961): p. 732.
20. K. Nobe, R.F. Tobias, Corrosion 20 (1964): p. 263t.
21. R.J. Chin, K. Nobe, J. Electrochem. Soc. 119 (1972): p. 1,457.
22. H.C. Kuo, K. Nobe, J. Electrochem. Soc. 125 (1978): p. 853.
23. E. McCafferty, N. Hackerman, J. Electrochem. Soc. 119 (1972): p. 999.
24. M. Jesionek, Z. Szklarska-Smialowska, Corros. Sci. 23 (1983): p. 183.
25. V.J. Drazic, D.M. Drazic, J. Serb. Chem. Soc. 57 (1992): p. 917.
26. Lj. Vracar, D.M. Drazic, J. Electroanal. Chem. 339 (1992): p. 269.
27. U. Ebersbach, K. Schwabe, K. Ritter, Electrochim. Acta 12 (1967): p. 927.
28. N. Sato, T. Noda, K. Kudo, Electrochim. Acta 19 (1974): p. 471.
29. P. Lorbeer, W.J. Lorenz, Corros. Sci. 21 (1981): p. 79.
30. P. Lorbeer, K. Jtittner, W.J. Lorenz, Werkst. Korros. 34 (1983): p. 290.
31. K.E. Heusler, K.G. Weil, K.F. Bonhoeffer, Z. Physik. Chem. 15 (1958): p. 149.
32. L.P. Mack, K. Nobe, Corrosion 40 (1984): p. 215.
33. K.J. Vetter, Z. Elektrochem. 59 (1955): p. 67.
34. M.A. Blesa, P.J. Morando, A.E. Regazzoni, Chemical Dissolution of Metal Oxides (Boca Raton, FL: CRC Press, 1994), p. 172.
35. K.J. Vetter, F. Gorn, Electrochim. Acta 18 (1973): p. 321.
36. K.E. Heusler, Corros. Sci. 29 (1989): p. 131.
37. J.O'M. Bockris, M.A. Genshaw, V. Brusic, H. Wroblowa, Electrochim. Acta 16 (1971): p. 1,859.
38. K.E. Heusler, B. Kusian, D. McPhail, Ber. Bunsenges. Phys. Chem. 94 (1990): p. 1,443.
39. B.D. Craig, D.S. Anderson, eds., Handbook of Corrosion Data (Materials Park, OH: ASM Int., 1995).
40. P.B. Mathur, T. Vasudevan, Corrosion 38 (1982): p. 171.
41. A. Anderko, M.M. Lencka, "Speciation Modeling of Advanced LiBr Absorption Cooling Fluids," Topical Technical Report no. GRI-97/0027 (Chicago, IL: Gas Research Institute, 1997).
42. K. Tanno, M. Itoh, H. Sekiya, H. Yashiro, N. Kuinagai, Corros. Sci. 34 (1993): p. 1,453.
43. K.F. Dockus, R.H. Krueger, W.F. Rush, ASHRAE J. 12 (1962): p. 67.
44. M.A. Stranick, Corrosion 40 (1984): p. 296.
45. E.A. Lizlovs, Corrosion 32 (1976): p. 263.
46. M.S. Vukasovich, "Molybdate: The Versatile Inhibitor," in Reviews on Corrosion Science and Technology, eds. A. Rainan, P. Labine (Houston, TX: NACE International, 1993), p. 11-12-I.
47. M.-H. Ahn, K.-K. Baek, "Evaluation of Combined Effect of Organic and Inorganic Inhibitors on the Metals Used in Absorption Refrigeration System," CORROSION/99, paper no. 97 (Houston, TX: NACE, 1999).
48. A. Cohen, R.V. Jelinek, Corrosion 22 (1966): p. 39.
49. Z. Szklarska-Smialowska, R. Staehle, J. Electrochem. Soc. 121 (1974): p. 1,393.
50. H.C. Helgeson, D.H. Kirkham, G.C. Flowers, Am. J. Sci. 281 (1981): p. 1,249.
51. J.C. Tanger, H.C. Helgeson, Am. J. Sci. 288 (1988): p. 19.
52. L.A. Bromley, AIChE J. 19 (1973): p. 313.
53. K.S. Pitzer, J. Phys. Chem. 77 (1973): p. 268.
54. G. Soave, Chem. Eng. Sci. 27 (1972): p. 1,197.
55. H.P. Meissner, ACS Symp. Ser. 133 (1980): p. 495.
56. F.P. Berger, K.-F.F.L. Hau, Int. J. Heat Mass Trans. 20 (1977): p. 1,185.
57. M.K. Fedorov, N.A. Antonov, S.N. Lvov, Russ. J. Appl. Chem. 49 (1976): p. 1,263.
58. D.A. Boryta, J. Chem. Eng. Data 20 (1973): p. 316.
59. K. Murakami, H. Sato, K. Watanabe, Int. J. Thermophys. 16 (1995): p. 811.
60. T. Ueinura, S. Hasaba, Technol. Rep. Kansai Univ. 6 (1964): p. 31.
61. W. Pennington, Refrig. Eng. (1955): p. 57.
62. J.J. Kessis, Bull. Soc. Chim. (1965): p. 48.
63. D.A. Boryta, J. Chem. Eng. Data 15 (1970): p. 142.
64. C.O. Adegoke, Int. J. Refrig. 16 (1993): p. 45.
65. R.T. Ellington, G. Kunst, R.E. Peck, J.F. Reed, "The Absorption Cooling Process," Inst. Gas. Technol. Res. Bull., no. 14 (Chicago, IL: Institute of Gas Technology, 1957).

APPENDIX A: THERMODYNAMIC FRAMEWORK

In a multicomponent system, the partial molal Gibbs energy of the i-th species is related to the molality (m_i) by:

$$\overline{G_i} = \overline{G_i^0} + RT \ln m_i \gamma_i \qquad (A-1)$$

where $\overline{G}_i^0$ is the standard-state partial Gibbs energy and γ_i is the activity coefficient. Thus, the thermodynamic properties of the system can be calculated if the standard-state Gibbs energies are available for all species as functions of temperature and pressure (i.e., $\overline{G}_i^0$ [T,P]) and the activity coefficients are known as functions of the composition vector (m) and temperature (i.e., γ_i[m,T]). From basic thermodynamics, the standard-state Gibbs energy of formation $\overline{G}_i^0$ (T,P) can be calculated as a function of temperature and pressure if the following data are available:

— Gibbs energy of formation at a reference temperature and pressure (usually, T_r = 298.15 K and P_r = 1 bar);

— Enthalpy of formation at T_r and P_r;

— Entropy at T_r and P_r;

— Heat capacity as a function of temperature and pressure; and

— Volume as a function of temperature and pressure.

The key to representing the standard-state properties over substantial temperature and pressure ranges is the accurate knowledge of the heat capacity and volume as functions of temperature and pressure. Then, the Gibbs energy and remaining functions can be obtained by integration using standard thermodynamic formulas. To express the temperature and pressure dependence of standard-state thermodynamic properties of aqueous species, the Helgeson-Kirkhain-Flowers-Tanger (HKFT) equation of state is used.[50-51] The HKFT equation is based on the solvation theory and expresses the standard-state thermodynamic functions as sums of structural and solvation contributions, the latter being dependent on properties of the solvent (i.e., water). In its revised form, the HKFT equation is capable of reproducing the standard-state properties up to 1,000°C and 5 kbar.[51] Expressions for the standard-state thermodynamic functions are given in the original papers[51] and are summarized in a review.[6]

The activity coefficient model used for representing the solution nonideality is an extended form of an expression developed by Bromley.[52] The extended Bromley equation is a combination of the Debye-Hückel term for long-range electrostatic interactions and a semi-empirical expression for short-range interactions between cations and anions. In a multicomponent system, the activity coefficient of an ion (i) is given by:

$$\log \gamma_i = \frac{-Az_i^2 I^{1/2}}{1+I^{1/2}} + \sum_j^{NO}\left[\frac{|z_i|+|z_j|}{2}\right]^2\left[\frac{(0.06+0.6B_{ij})|z_i z_j|}{\left(1+\frac{1.5}{|z_i z_j|}I\right)^2}+B_{ij}+C_{ij}I+D_{ij}I^2\right]m_j \quad \text{(A-2)}$$

where A is the Debye-Hückel coefficient that depends on temperature and solvent properties; z_i is the number of charges on i; I is the ionic strength (i.e., $I = 0.5\sum z_i^2 m_i$); NO is the number of ions with charges opposite to that of i; and B_{ij}, C_{ij}, D_{ij} are empirical, temperature-dependent, cation-anion interaction parameters. Bromley's original formulation contains only one interaction parameter, B_{ij}, which is sufficient for systems with moderate ionic strength.[52] For concentrated systems, the two additional coefficients, C_{ij} and D_{ij}, usually become necessary. The three-parameter form of the Bromley model is capable of reproducing activity coefficients in solutions with very high ionic strengths, which cover the composition range of refrigeration working fluids. The temperature dependence of the B_{ij}, C_{ij}, and D_{ij} usually is expressed using a simple quadratic function.

The Bromley model is restricted to interactions between cations and anions. For ion-molecule and molecule-molecule interactions, the well-known model by Pitzer is used.[53] To calculate fugacities of components in the gas phase, the Redlich-Kwong-Soave equation of state is used.[54]

In the absence of sufficient experimental data, reasonable predictions can be made using a method by Meissner, which makes it possible to extrapolate activity coefficients to higher ionic strengths based on only a single, experimental or predicted data point.[55]

APPENDIX B: CALCULATION OF THE MASS TRANSFER COEFFICIENT

The mass transfer coefficient (k_m) can be calculated once the flow geometry is assumed (Equation [13]). For example, analytical expressions are available for the rotating disk, rotating cylinder, and pipe flow geometries. For practical calculations, the pipe flow geometry is particularly important. The k_m can be expressed in terms of the dimensionless Reynolds (Re) and Schmidt (Sc) numbers. These numbers are defined by:

$$\mathrm{Re} = \frac{vd}{\nu} \quad \text{(B-1)}$$

$$\mathrm{Sc} = \frac{\nu}{D} \quad \text{(B-2)}$$

where v is the linear velocity, ν is the kinematic viscosity, D is the diffusion coefficient of the species that undergoes the electrochemical reaction, and d is the diameter. The diffusion coefficient and viscosity are calculated as functions of temperature and concentration using methods developed by Anderko and Lencka[8] and Lencka, et al.,[7] respectively. After computing the Re and Sc numbers, the mass transfer coefficient for single-phase flow in a straight pipe can be computed using the correlation of Berger and Hau:[56]

$$\frac{k_m d}{D} = 0.0165\,\mathrm{Re}^{0.86}\,\mathrm{Sc}^{0.33} \quad \text{(B-3)}$$

Access The World's Most Complete Source Of Corrosion Bibliographic Information Via The Internet!

Introducing...

CORROSION ABSTRACTS DATABASE ON THE NET

With the rapid evolution of the Internet as a primary source for technical information, NACE International and Cambridge Scientific Abstracts have teamed up to bring you Corrosion Abstracts Database on the World Wide Web.

Corrosion Abstracts Database provides engineers and scientists with a resource for solving corrosion problems by reviewing the documented experience of others, and by providing summarized findings in the article abstracts. **The database includes more than 74,000 abstracts dating back to 1980 from more than 150 sources worldwide**. The abstracts cover the areas of general corrosion, testing, corrosion characteristics, preventative measures, materials construction and performance, and equipment for many industries.

About Cambridge Scientific Abstracts & the Internet Database Service (IDS):

Publishing for over 40 years, Cambridge Scientific Abstracts provides a wide range of scientific and technical journals and databases including Metals Abstracts and METADEX. Their Internet Database Service IDS provides access to scientific databases via the Internet's World Wide Web featuring monthly updates and extensive backfile archives.

The print edition of Corrosion Abstracts is also published by Cambridge Scientific Abstracts in cooperation with NACE International.

Visit the award-winning Internet Database Service at www.csa.com.

Subscribing to Corrosion Abstracts Database yields maximum benefits quickly and easily!

- **Significantly reduced prices** — *you can access the same information contained in the printed journal and the COR*AB CD-ROM at significantly reduced prices*
- **Instant 24-hour access** — *simply log on to the Internet*
- **Current, up-to-date information** — *you no longer have to wait for bimonthly updates*
- **Computerized literature searches** — *you no longer have to flip through volumes of printed journals*

Benefits Exclusive to NACE Members:

- NACE Members receive further reduced prices
- Gold, Silver, and Bronze NACE Member Representatives receive complimentary access to the corresponding current-year records and a one-year backfile on IDS (through 1998).
- Corporate Members receive discounted rates to Cambridge Scientific Abstract's extensive Materials Collection Database available through IDS.

NACE Member Prices:

Only 2¢ Per Abstract!

Item #38169 $69 per year
For the current year of Corrosion Abstracts Database — ***ONLY AVAILABLE TO NACE MEMBERS!***

Item #38170 $149 per year
For the entire Corrosion Abstracts Database - dating back to 1980

Item #38171 $947 per year
For a site license of the entire Corrosion Abstracts Database

List Prices for Non-Members:

Item #38172 $199 per year
For the entire Corrosion Abstracts Database - dating back to 1980

Item #38173 $1250 per year
For a site license of the entire Corrosion Abstracts Database

30-Day Money Back Guarantee!
To subscribe to Corrosion Abstracts Database, please contact NACE Membership Services by phone at 281/228-6223, by fax 281/228-6300, or send an E-mail to msd@mail.nace.org.

NACE INTERNATIONAL
THE CORROSION SOCIETY

Abbreviated Instructions for *Corrosion* Authors[1]

The following basic guidelines are to be followed in preparing manuscripts for publication in *Corrosion*.

SUBMISSION

Manuscripts may be submitted on computer diskette with hard copies and original graphics attached, or on paper in typewritten form.

Three copies of the text plus **one original and two copies** of all graphics should be sent to *Corrosion* Technical Editor, Dr. J.B. Lumsden, Rockwell International Science Center, 1049 Camino Dos Rios, PO Box 1085, Thousand Oaks, CA 91360.

GENERAL STYLE REQUIREMENTS

Abbreviations, acronyms, and symbols must be identified upon first use by spelling completely the word or term and following it with the abbreviation, acronym, or symbol in parentheses. The abbreviation, acronym, or symbol then must be used consistently throughout the publication.

Abbreviations of periodicals must be used consistently, particularly in reference lists. Abbreviations for other periodicals should be consistent (e.g., J. always should be used as the abbreviation for Journal; Chem. always should be used for Chemistry; Int. always should be used for International, etc.). Abbreviated periodical titles in reference lists must not be italicized or underlined.

Standard, recommended practice, test method, and material requirements must be capitalized when referring to specific NACE standards by designation, but not when referring to classifications of standards (NACE's or others') in general (i.e., Testing shall conform to the requirements of NACE Standard TM0177-90, "Testing of Metals for Resistance to Sulfide Stress Cracking at Ambient Temperatures." This test method may be supplemented with tests from other standards as required by the user.)

Specific units of a publication, excluding pages, should be capitalized when cited within the text, as in Section 2, Foreword, Figure 2, Table 2, Equation (4).

Specific specimens, classes, grades, tests, and other such units should be capitalized when they are cited within the text (Specimen A, Class C, Grade 60, Test 3).

Every effort must be made to use generic names in place of trade names. UNS designations, specification numbers, or chemical compositions must be used in place of materials trade names.

All equations, figures, and tables must be numbered consecutively throughout the text (e.g., Equation [1], Figure 2, Table 4). Equations should be placed consecutively throughout the text, centered on a separate line. Place all tables and figures at the end of the text, numbered consecutively on separate sheets (with the primary author's name and manuscript number).

[1] The *Corrosion Author's Guide* and *NACE Publications Style Manual* should be used for more complete instructions and guidelines for submitting and preparing a manuscript for publication in *Corrosion*. The guide and style manual can be obtained free from NACE International, PO Box 218340, Houston, TX 77218-8340; phone: 281/228-6223: fax: 281/228-6329; or by visiting www.nace.org. Questions and concerns about papers should be directed to the Managing Editor, phone: 281/228-6200; fax: 281/228-6300; or e-mail: angelaj@mail.nace.org.

GRAPHICS

Submit a **copy** of all artwork, line drawings, and photographs with all labeling or lettering indicated, and **one original without type, labeling, lettering, or legends of any kind**. Do not paste, tape, or otherwise affix any labels or lettering to the original artwork itself. NACE staff will reset our type to uniform specifications, using the labeled copy as a guide.

Submit all electronic artwork in BMP, JPEG, TIFF, WMF, PDF, or EPS file formats or in their original computer software drawing format if the package is one of the following: Macromedia FreeHand†, Adobe Illustrator†, Microsoft PowerPoint†, Adobe Photoshop†, CorelDraw†, or Lotus Freelance Plus†. Electronic images of all types of artwork must have a minimum resolution of 300 dots per inch (dpi).

Do not use gradient screens (different shades of the same basic color) within line drawings or attached to photographs to indicate a range of values.

Thermal prints, dot-matrix prints, fax copies, and photocopies are not acceptable, except as a backup reference for electronic files.

REFERENCES

References must be noted in the text by a superscript Arabic numeral and numbered consecutively throughout the publication.

The list of references appears after the main body of text, with the references appearing in numerical order.

To avoid interrupting the flow of thought of a sentence, reference and footnote numbers preferably are placed after any punctuation, except a dash, and preferably at the end of a sentence.

The main facts in references are separated by commas and should be consistent in order, content, and punctuation with the examples listed in the *NACE Publications Style Manual, Appendix G.*

Books

1. A.G. Ostroff, Introduction to Oilfield Water Technology (Houston, TX: NACE International, 1979), p. 17.

Periodical Articles

12. J.-L. Crolet, M.R. Bonis, Corrosion 56, 2 (2000): p. 167. (*Issue number is not necessary if journal page numbers are continuous throughout the volume.*)

Proceedings

17. R.H. Hausler, ed., Corrosion Inhibition—Proceedings of the International Conference on Corrosion Inhibitors, held May 16-20, 1983 (Houston, TX: NACE, 1988), p. 68.

Standards

20. NACE Standard RP0170-93, "Protection of Austenitic Stainless Steels and Other Austenitic Alloys from Polythionic Acid Stress Corrosion Cracking During Shutdown of Refinery Equipment" (Houston, TX: NACE, 1993).

Conference Papers

25. H. Zeisel, F. Durst, "Computations of Erosion-Corrosion Processes in Separated Two-Phase Flows," CORROSION/90, paper no. 29 (Houston, TX: NACE. 1990).